Robust Stability Analysis of the Space Launch System Control Design: A Singular Value Approach

Jing Pei[1]
NASA Langley Research Center, Hampton VA 23681

Jerry R. Newsom[2]
Analytical Mechanics Associates, Hampton VA 23681

Classical stability analysis consists of breaking the feedback loops one at a time and determining separately how much gain or phase variations would destabilize the stable nominal feedback system. For typical launch vehicle control design, classical control techniques are generally employed. In addition to stability margins, frequency domain Monte Carlo methods are used to evaluate the robustness of the design. However, such techniques were developed for Single-Input-Single-Output (SISO) systems and do not take into consideration the off-diagonal terms in the transfer function matrix of Multi-Input-Multi-Output (MIMO) systems. Robust stability analysis techniques such as H_∞ and μ are applicable to MIMO systems but have not been adopted as standard practices within the launch vehicle controls community. This paper took advantage of a simple singular-value-based MIMO stability margin evaluation method based on work done by Mukhopadhyay and Newsom and applied it to the SLS high-fidelity dynamics model. The method computes a simultaneous multi-loop gain and phase margin that could be related back to classical margins. The results presented in this paper suggest that for the SLS system, traditional SISO stability margins are similar to the MIMO margins. This additional level of verification provides confidence in the robustness of the control design.

Note to readers: the axes labels were taken off some figures to meet International Traffic in Arms Regulations (ITAR) requirements.

Nomenclature

K_n	= Gain variation
φ_n	= Phase variation
L	= Uncertainty matrix
KG	= Open loop transfer function matrix
$\underline{\sigma}$	= Minimum Singular value
$\overline{\sigma}$	= Maximum Singular value
$K_{n,SISO,aero}$	= Smallest SISO aerodynamic gain margin
$K_{n,MIMO,aero}$	= Equivalent MIMO aerodynamic gain margin
$K_{n,SISO,RB}$	= Smallest SISO rigid body gain margin
$K_{n,MIMO,RB}$	= Equivalent MIMO rigid body gain margin
$K_{n,SISO,simul}$ & $\varphi_{n,SISO,simul}$	= Smallest SISO simultaneous gain and phase margins
$K_{n,MIMO,simul}$ & $\varphi_{n,MIMO,simul}$	= Equivalent MIMO simultaneous gain and phase margins
$\omega_{SISO,RB}$	= Frequency that corresponds to $K_{n,SISO,RB}$
$\omega_{SISO,aero}$	= Frequency that corresponds to $K_{n,SISO,aero}$
$\omega_{MIMO,simul}$	= Frequency that corresponds to the minimum singular value of the MIMO system

[1] Aerospace Engineer, Systems Analysis and Concepts Directorate, Vehicle Analysis Branch
[2] Aerospace Engineer, Research Directorate, Dynamic Systems and Control Branch

I. Introduction

The design of NASA's Space Launch System (SLS) vehicle[2] represents a challenging task that requires careful tradeoff between maximizing rigid body performance while stabilizing effects such as fluid slosh and flexible dynamics with adequate margins. The standard flight heritage architecture of integrating a PID controller with a linear bending filter is the traditional choice for large launch vehicles. The controller gains and filters are optimized assuming decoupling in roll, pitch, and yaw. This assumption is valid considering the inertial coupling and aerodynamic cross-axis coupling terms are generally small for launch vehicles. Under the assumption that the SLS time-varying dynamics and control system can be frozen over a short period of time and linearized, classical stability techniques such as Root Locus, Nyquist, and Nichols are used to evaluate the stability margins of the system.

Gain and phase margins results from classical methods are a form of unstructured uncertainty[3]. They indicate how much gain or phase variations at specific crossover frequencies can be tolerated before the closed loop system becomes unstable. Typical designs employ 6 dB and 30 degrees of gain and phase margin requirements. For dispersed frequency domain Monte Carlo analysis[4] those metrics can be reduced to 3 dB and 20 degrees respectively.

Stability robustness analysis aims to measure how model parameter variations or uncertainties affect the stability of the feedback system. Structured singular value techniques developed by Doyle[5] provide control engineers with a guideline on how to quantify the robust stability of a multivariable feedback system. Mukhopadhyay and Newsom[1] described a simple stability margin evaluation method that relates the singular values of the return difference matrix to simultaneous gain and phase changes in all loops of a multi-loop system. Works by Yeh[6] and Anderson[7] follow a similar approach and apply the method to an aircraft model with as many as 8 states. The SLS open-loop compensated system (controller and plant) carries as many as 500 states at a given operating condition. Reducing the model via linear fractional transformation[8] and performing rigorous μ analysis is time consuming and may not yield results that are intuitive. The approach described by Mukhopadhyay and Newsom offers a quick and simple way of assessing the stability robustness of the nominal multivariable feedback system that can be directly related back to classical stability margins. The method is equivalent to having all the direct and cross-feed transfer functions varied simultaneously in the worst-case direction. The worst-case variations in all loops is an extreme case, hence the results generally tend to be conservative.

The purpose of this paper is to apply the method described in[1] that uses singular values to evaluate the robustness of the SLS control system from a MIMO perspective. The paper is organized as follows: Section 1 provides the reader with motivation behind this study. Section 2 offers relevant background information. Section 3 describes the general approach behind this analysis. Section 4 applies this method to a simple 2x2 MIMO academic model of a launch vehicle. Section 5 shows results using the high-fidelity SLS simulation model and highlights the comparisons between MIMO and SISO stability margins. Section 6 concludes the discussion and summarizes the findings.

II. Background

In addition to the standard gain and phase margin requirements, a Nichols disc margin metric is used to evaluate the closest approach on the Nichols space as shown in Fig. 1. The SLS vehicle is a conditionally stable system; the aerodynamic and rigid body gain margins represent the range of loop gain the system must operate to maintain stability. The concept of disc margin can be thought of as how much simultaneous gain and phase variations a single loop can accommodate before becoming unstable. The disc is anchored at the critical point (0 dB, -180 deg) with semi and major axes being the classical gain and phase margin requirements. If any part of the frequency response enters the disc then the design is deemed to have been violated. Disc margin is a better approach for determining acceptable variations because in general real life uncertainties do not occur in the form of a gain or phase variation nor do they occur only at specific frequencies. A nonlinear analytical mapping can be used to convert the Nichols disc margin to the Nyquist plane shown in Fig. 2. Once in the Nyquist plane, the ellipse is no longer symmetric with respect to the critical point (-1, 0).

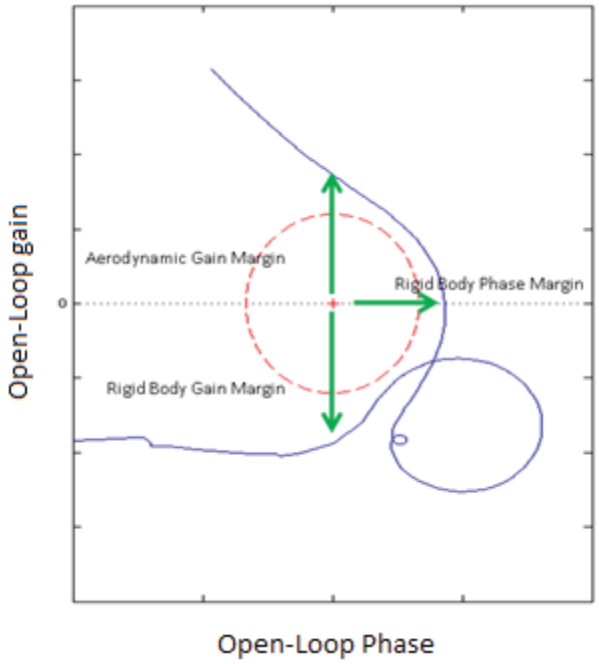

Figure 1. Nichols Chart Definition

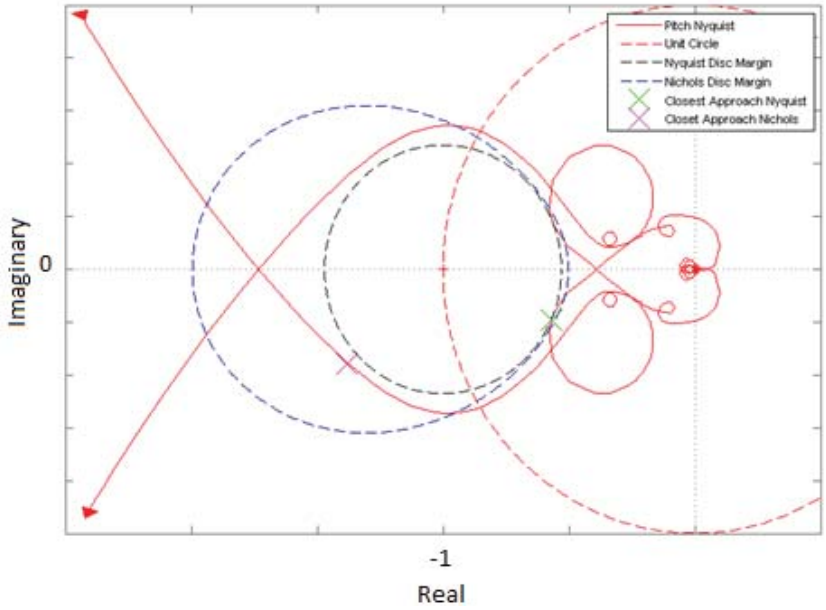

Figure 2. Nyquist Plot with Disc Margin

Despite the numerous frequency domain margin requirements, the major drawback to classical techniques is that they apply only to time-invariant SISO systems. In Nyquist array analysis[3], the radius of each Gershgorin circle depends on the entire column or row of the transfer function matrix (TFM). Ignoring interaction between different elements of the TFM can produce misleading stability results. For MIMO systems, the closed loop characteristic equation ($I+KG$) is no longer a scalar but a matrix. The generalized Nyquist stability criterion[3] shown by Eq. (1)

states that the MIMO feedback system is stable if and only if the number of counter-clockwise encirclements P_c, of the critical point (the origin) by the contour det(I+KG) is equal to the number of unstable open-loop poles P_o.

$$\Delta \arg \det\left[I + KG(j\omega)\right] = -2\pi\left(P_c - P_o\right) \tag{1}$$

Figure 3 is a sample MIMO Nyquist diagram. As oppose to SISO systems, the shortcoming of plotting the determinate locus on the *s-plane* of a MIMO system and inspecting the distance to the critical point is that it is not always a good representation of relative stability margin.

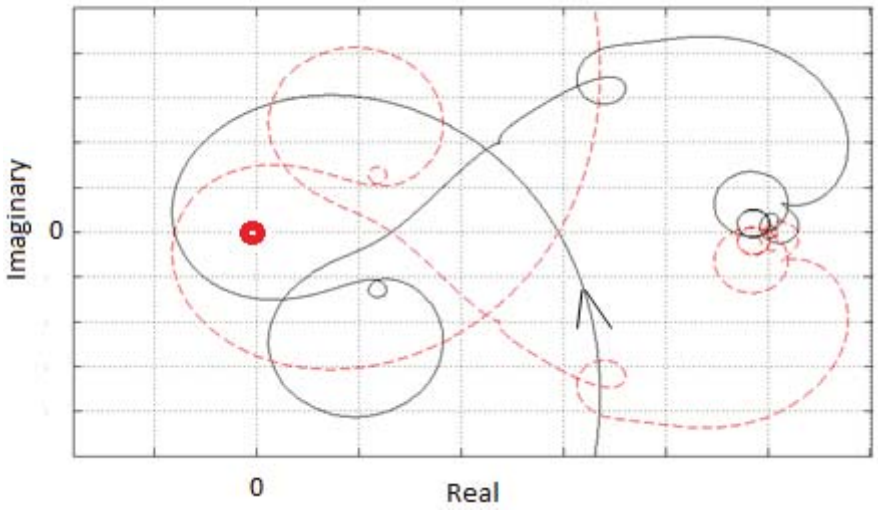

Figure 3. MIMO Nyquist Plot

III. Approach

The approach in Mukhopadhyay and Newsom[1] relates the minimum singular value ($\underline{\sigma}$) of the return difference matrix (I+KG) to gain (K_n) and phase variations (φ_n) in all loops (roll, pitch, and yaw for the SLS system) simultaneously. Figure 4 is a simplified block diagram, where KG represents the nominal 3x3 open loop transfer function matrix (OLTFM) and L represents the 3x3 diagonal complex gain uncertainty matrix composed of K_n and φ_n shown in Eq 2. The derivation in relating $\underline{\sigma}$ of the return difference matrix of the nominal system to gain and phase variations can be summarized as follows. The detailed derivation can be found in[1].

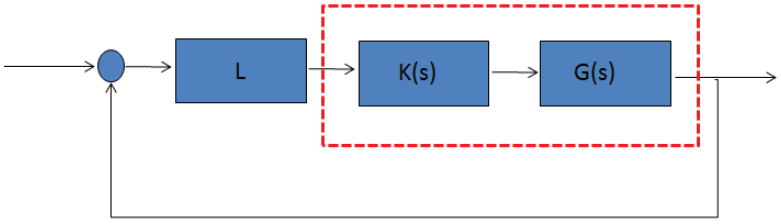

Figure 4. Schematic of General Approach

$$L = \begin{bmatrix} K_n e^{-j\varphi_n} & 0 & 0 \\ 0 & K_n e^{-j\varphi_n} & 0 \\ 0 & 0 & K_n e^{-j\varphi_n} \end{bmatrix} \tag{2}$$

The nominal closed-loop system is assumed to be stable. Therefore:

$$\det\left(I + KG(j\omega)\right) \neq 0 \quad or \quad \underline{\sigma}\left(I + KG(j\omega)\right) > 0 \tag{3}$$

Stability of the perturbed system is guaranteed if:

$$\underline{\sigma}\left(I + LKG\right) > 0 \tag{4}$$

The matrix L is separated from G by the following identity:

$$I + LKG = \left[\left(L^{-1} - I\right)\left(I + KG\right)^{-1} + I\right]\left(I + KG\right)L \tag{5}$$

L and $I+KG$ are nonsingular, therefore $I+LKG$ is nonsingular if and only if $\left(L^{-1} - I\right)\left(I + KG\right)^{-1} + I$ is nonsingular. It can be shown after applying a few singular value properties[6,7] that the stability of the perturbed system is guaranteed if:

$$\bar{\sigma}\left(L^{-1} - I\right) < \underline{\sigma}\left(I + KG\right) \tag{6}$$

where:

$$\bar{\sigma}\left(L^{-1} - I\right) = \sqrt{\left(1 - \frac{1}{K_n}\right)^2 + \frac{2}{K_n}\left(1 - \cos\varphi_n\right)}$$

As a result, the nominal closed-loop system is stable if:

$$\underline{\sigma}\left(I + KG\right) \geq \sqrt{\left(1 - \frac{1}{K_n}\right)^2 + \frac{2}{K_n}\left(1 - \cos\varphi_n\right)} \tag{7}$$

The minimum singular value of a square matrix is a measure of the distance to singularity. If $\underline{\sigma}$ of the return difference matrix approaches zero, the closed-loop system is near a stability boundary. The inequality constraint in Eq. (7) holds for all ω, except at ω_o (frequency where $\underline{\sigma}$ occurs) . Equality in the expression is satisfied at ω_o. The system under this perturbation will have a pair of closed-loop poles at +/- $j\omega_o$. Whether the system goes from stable to unstable or vice versa requires further examination of the MIMO Nyquist plot. In this study the nominal closed-loop system is assumed to be stable. Figures 5 and 6 illustrate the solutions to Eq. (7). It is important to note that for a given $\underline{\sigma}$ there are many combinations of K_n and φ_n that satisfy Eq. (7) but fail to destabilize the system. which highlights the conservatism behind this approach.

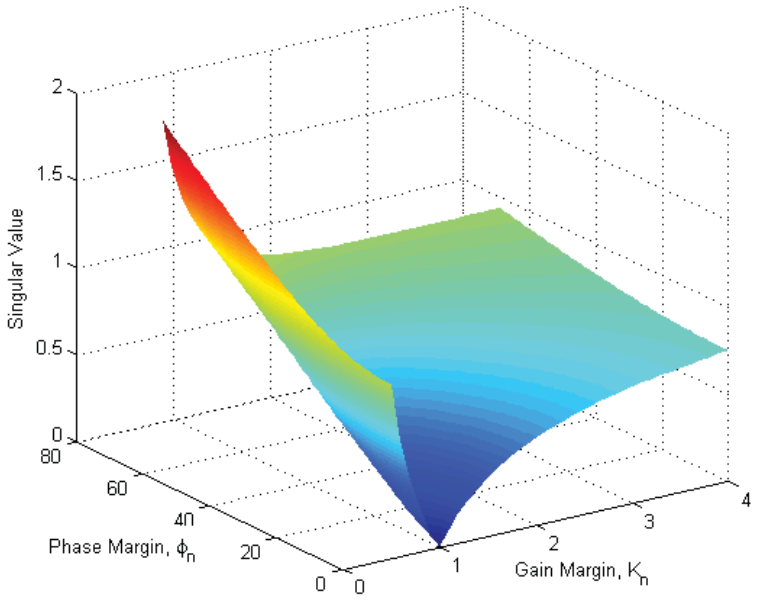

Figure 5. Contour Plot Relating φ_n and K_n to σ

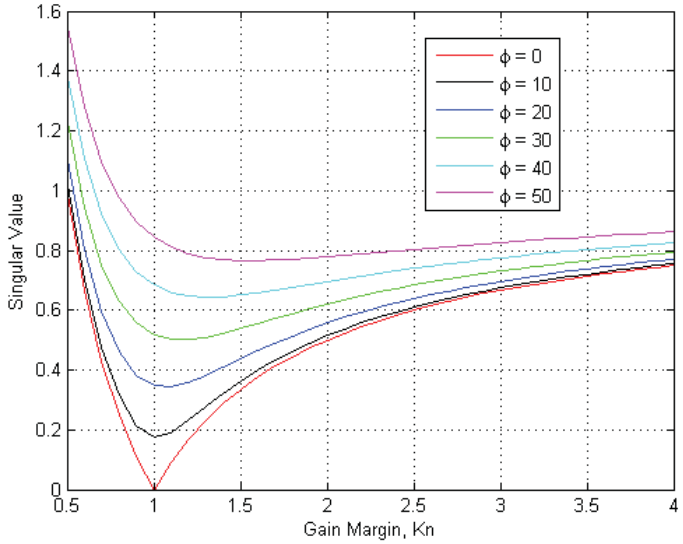

Figure 6. Line Plot Relating φ_n and K_n to σ

IV. Application to Simple Dynamics Model

In this section, the method described in Section II is applied to a simple dynamics model of a launch vehicle. The intention to provide additional insight into the approach before applying it to a more complicated system. The model consists of unstable pitch and yaw rotational modes, two 3rd order actuator dynamics models, and a 2nd order structural dynamics model that exhibits non-planar bending characteristics. Separate PD controllers are designed to stabilize the rigid body in pitch and yaw, which amounts to a conditionally stable 2x2 MIMO system. Rigid body cross-axis coupling is represented by the aerodynamic terms Cm_β and Cn_α. Figure 7 shows the Nichols plot of the nominal system without any rigid body coupling. The worst-case SISO aerodynamic gain margin, $K_{n,SISO,aero}$ occurs in the pitch channel (1,1 term) with a value of -19 dB. Equation 7 was used to obtain an equivalent MIMO

aerodynamic gain margin, $K_{n,MIMO,aero}$. As expected, $K_{n,MIMO,aero}$ and $K_{n,SISO,aero}$ have the same value due to the lack of coupling at low frequency. As a check, $K_{n,MIMO,aero}$ and $K_{n,SISO,aero}$ were separately substituted into the matrix L shown in Eq. (2). In both cases, one of the pitch rigid body closed-loop poles became neutrally stable.

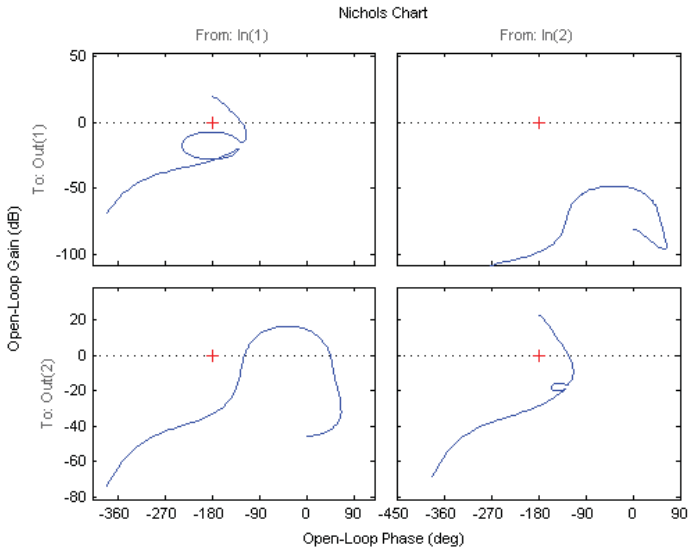

Figure 7. Nichols Chart of Simple Dynamics Model

As the next step, the level of rigid body coupling was augmented by significantly increasing the Cm_{β} and Cn_{α}. This caused $K_{n,MIMO,aero}$ to decrease to -16.8 dB. Substitution of $K_{n,SISO,aero}$ into the matrix L caused one of the rigid body poles to move well into the right-hand *s-plane* (RHP). In contrast, $K_{n,MIMO,aero}$ ensured that pole was kept stable. This illustrates the well-known fact that SISO margins are not adequate in capturing the stability of a MIMO system when there are significant coupling dynamics present. The MIMO margin provides a more conservative result.

V. Simulation Results

In this section, the evaluation method is applied to the high-fidelity dynamic model of the SLS vehicle. The Space Transportation Analysis Research Simulation (STARS)[9], developed at NASA Langley Research Center, was used to generate the nominal OLTFM at various times in the trajectory. Numerical linearization of the nonlinear *Simulink* model was used to create the linear state space models. The loop was broken at the output of the flight control system to obtain the 3x3 OLTFM. An example of the return difference matrix $I+KG$ singular values is shown in Fig. 8. The objective is to determine MIMO gain margins ($K_{n,MIMO,RB}$ and $K_{n,MIMO,aero}$) and simultaneous MIMO gain and phase margins ($K_{n,MIMO,simul}$ & $\varphi_{n,MIMO,simul}$) using the minimum singular value curve at various critical frequencies through Eq. (7).

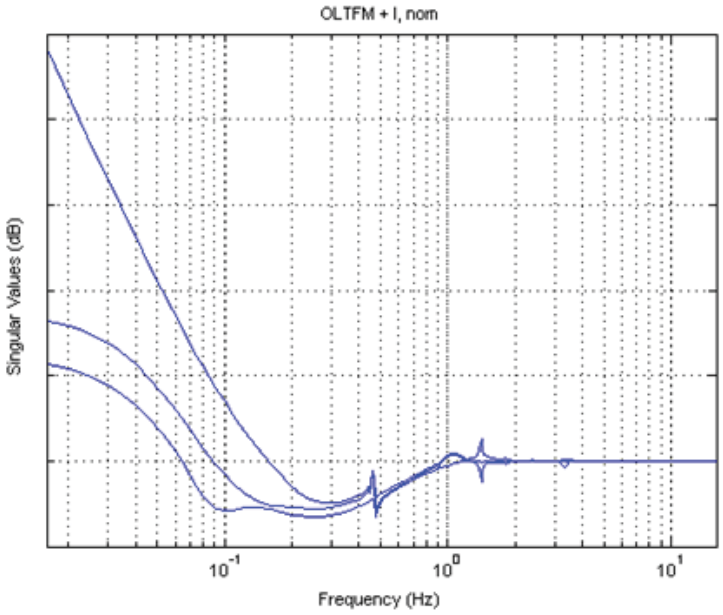

Figure 8. MIMO Return Difference Singular Value Plot

Figure 9 is a comparison of the worst-case SISO rigid body gain margin, $K_{n,SISO,RB}$ to the MIMO rigid body gain margin, $K_{n,MIMO,RB}$. $K_{n,SISO,RB}$ is the channel (roll, pitch, or yaw) with the smallest gain margin at the second -180º phase crossing, $\omega_{SISO,RB}$. $K_{n,MIMO,RB}$ is determined by obtaining $\underline{\sigma}$ of the nominal return difference matrix at $\omega_{SISO,RB}$ and solving Eq. (7) for K_n with φ_n set to the nominal value of zero.

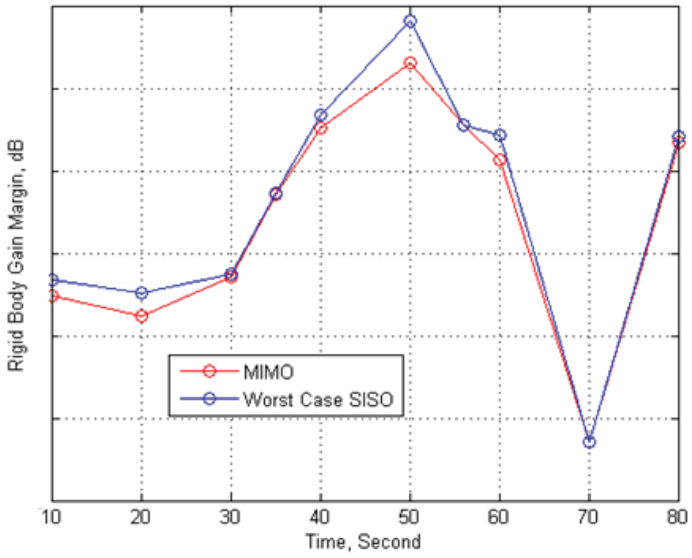

Figure 9. MIMO vs. Worst Case SISO Rigid Body Gain Margin

As a check, $K_{n,MIMO,RB}$ and $K_{n,SISO,RB}$ were separately substituted into the matrix L shown in Eq. (2). The pole-zero map of the perturbed system is shown in Fig. 10. The frequency of the complex pole in close proximity to the imaginary axis corresponds to $\omega_{SISO,RB}$. Depending on the dynamics of the linearized system, $K_{n,SISO,RB}$ at times causes that pole to shift slightly over to the RHP, whereas $K_{n,MIMO,RB}$ ensures that the pole never crosses the imaginary axis. It is apparent from Fig. 9 that $K_{n,MIMO,RB}$ is always more conservative compared to $K_{n,SISO,RB}$. Figure

11 is a similar plot comparing the worst-case SISO aerodynamic gain margin, $K_{n,SISO,aero}$ to the MIMO aerodynamic gain margin, $K_{n,MIMO,aero}$. Once again, the MIMO margins are more conservative.

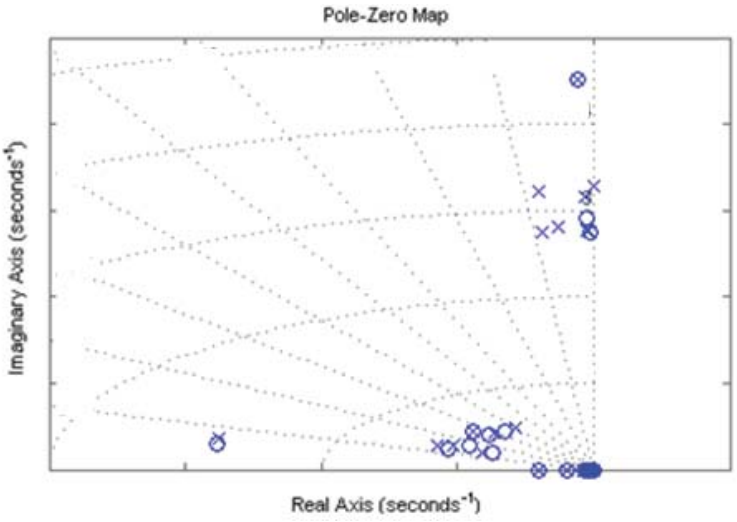

Figure 10. Closed-Loop Pole-Zero Map (magnified) of the Perturbed System

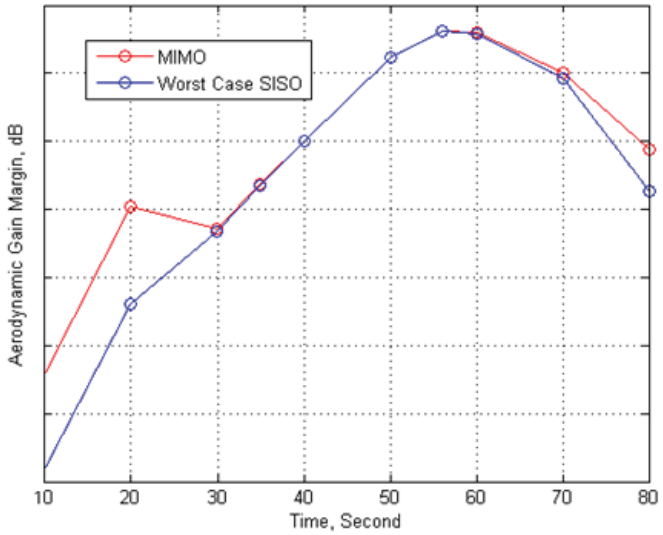

Figure 11. MIMO vs. Worst Case SISO Aerodynamic Gain Margin

Figure 12 illustrates SISO and MIMO simultaneous gain and phase margins. $K_{n,SISO,simul}$ and $\varphi_{n,SISO,simul}$ are obtained by the taking the loop with the closest approach on the Nyquist diagram and determining how much gain and phase variations would cause the curve to impinge on the critical point (-1,0). The closest approach on a SISO Nyquist diagram is consistent with the frequency at which $\underline{\sigma}$ occurs on the SISO return difference plot shown in Fig. 13. The closest approach occurs in the pitch channel at approximately 0.48 Hz.

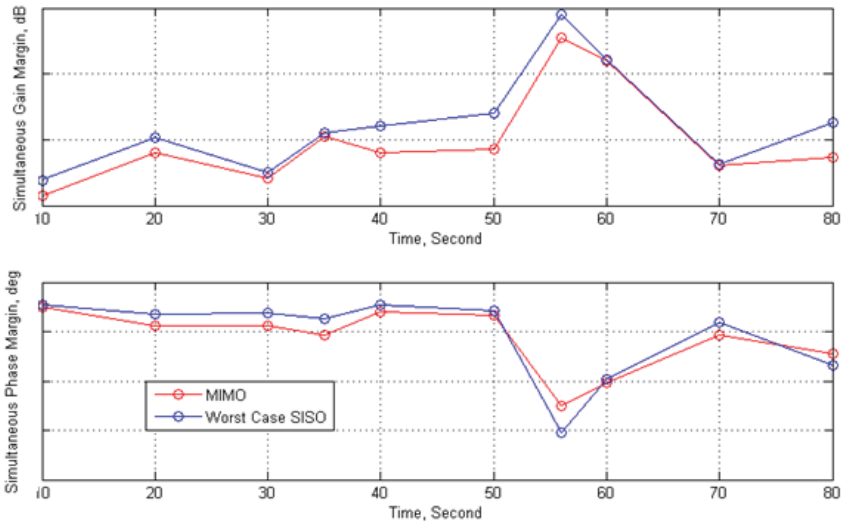

Figure 12. Simultaneous Gain and Phase Margins at Various Trajectory Times

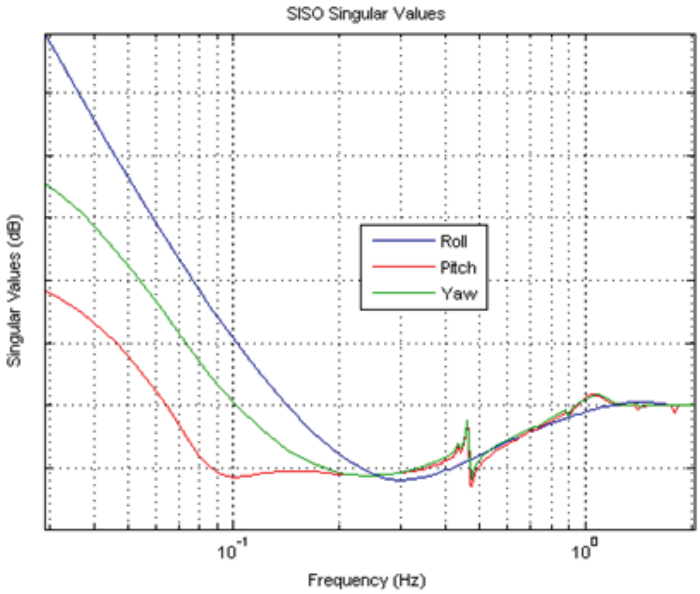

Figure 13. SISO Return Difference Singular Value Plot

$K_{n,MIMO,simul}$ and $\varphi_{n,MIMO,simul}$ are computed by obtaining $\underline{\sigma}$ of the MIMO return difference matrix shown in Fig. 8 and computing K_n and φ_n which satisfies Eq. (7) and causes the closed-loop pole at $\omega_{MIMO,simul}$ to be closest to the imaginary axis. Results from Fig. 12 are consistent with the gain-only results from Figs. 9 and 11. It shows that the MIMO margins are slightly more conservative compared to the SISO margins when applied to all 3 channels simultaneously. As a check, the MIMO and SISO gain and phase margins were once again substituted into the matrix L and the locations of the closed-loop poles were examined on the pole-zero map. The SISO margins caused the pole at the critical frequency to move slightly into the RHP, whereas the MIMO margins ensured that pole never crossed the imaginary axis.

Despite the slight differences, the overall magnitude and trend based on the MIMO analysis are very similar to the classical SISO results. For instance, both methods indicated that at T = 56 seconds the phase margin is the smallest

due to a combination of maximum aerodynamic instability and control-structure interaction constraints. Similarity between the two methods is expected due to the very small coupling associated with the SLS rigid-body dynamics. The MIMO results provide additional confidence that the classical margins are adequate in capturing the stability robustness of the SLS vehicle.

VI. Conclusion

In this paper, a multi-loop stability margin evaluation method was applied to the SLS vehicle. This technique offers a simple way to assess the stability of the MIMO system with results that could be directly related back to classical stability margins. Hence it serves as an excellent compliment to the classical methods. The MIMO margins were shown to be similar but slightly conservative compared to the SISO results due to the lack of cross coupling associated with the rigid-body dynamics. The similarity between the MIMO and SISO margins suggests that the classical stability evaluation method is adequate to capture the robustness of the control design for SLS.

References

[1] Mukhopadhyay, V., and Newsom, J., "Application of Matrix Singular Value Properties for Gain and Phase Margins of Multi-loop Systems," NASA TM-84524. July 1982.

[2] Orr, J., "Space Launch System Flight Control," Aerospace Control and Guidance Systems Committee (ACGSC), 10-12 Oct. 2012, Portland, ME.

[3] Maciejowski, J., *Multivariable Feedback Design*, 1st ed. Addison-Wesley Publishers, 1989.

[4] Jang, J., Tassel, C., Bedrossian, N., Hall, C., Spanos, P., "Evaluation of Ares I Control System Robustness to Uncertain Aerodynamic and Flex Dynamics," *AIAA GN&C Conference*, 18-21 Aug. 2008, Honolulu, Hawaii.

[5] Doyle, J.C., "Robustness of Multi-loop Linear Feedback System," *17th IEEE Conference on Decision and Control*, San Diego, Calif., Jan 1979, pp. 12-18.

[6] Yeh, H. Ridgely, D. Banda, S. "Nonconservative Evaluation of Uniform Stability Margins of Multivariable Feedback Systems". *Journal of Guidance, Control, and Dynamics*, Vol. 8, No 2, March-April 1985.

[7] Anderson, M. "Robustness Evaluation of a Flexible Aircraft Control System". *Journal of Guidance, Control, and Dynamics*, Vol. 16, No 3, May-June 1993.

[8] Green, M., Limebeer, D., *Linear Robust Control*. Pearson Education, Inc.

[9] "Space Transportation Analysis and Research Transportation Simulation". Dynamics & Control Branch. NASA Langley Research Center. 2013